Journal of Power Sources 185 (2008) 941–945

Contents lists available at ScienceDirect

Journal of Power Sources

journal homepage: www.elsevier.com/locate/jpowsour

Short communication

Pd nanoparticles supported on WO_3/C hybrid material as catalyst for oxygen reduction reaction

Zhonghua Zhang[a,b], Xiaogang Wang[a,b], Zhiming Cui[a,b], Changpeng Liu[a], Tianhong Lu[a], Wei Xing[a,*]

[a] State Key Laboratory of Electro-analytical Chemistry, Changchun Institute of Applied Chemistry, Chinese Academy of Sciences, Changchun 130022, PR China
[b] Graduate University of the Chinese Academy of Sciences, Beijing, PR China

ARTICLE INFO

Article history:
Received 19 May 2008
Received in revised form 5 July 2008
Accepted 7 July 2008
Available online 26 July 2008

Keywords:
Catalyst
Fuel cell
Oxygen reduction reaction
Pd–WO_3/C
Hydrogen tungsten bronze

ABSTRACT

Pd nanoparticles supported on WO_3/C hybrid material have been developed as the catalyst for the oxygen reduction reaction (ORR) in direct methanol fuel cells. The resultant Pd–WO_3/C catalyst has an ORR activity comparable to the commercial Pt/C catalyst and a higher activity than the Pd/C catalyst prepared with the same method. Based on the physical and electrochemical characterizations, the improvement in the catalytic performance may be attributed to the small particle sizes and uniform dispersion of Pd on the WO_3/C, the strong interaction between Pd and WO_3 and the formation of hydrogen tungsten bronze which effectively promote the direct 4-electron pathway of the ORR at Pd.

1. Introduction

Direct methanol fuel cells (DMFCs) are attracting more and more attention as environmentally friendly power sources for transportation and stationary applications. However, the commonly employed Nafion membrane suffers from serious methanol crossover, which not only lowers the fuel utilization efficiency but also adversely affects the cathode performance, and thus leads to a loss in the overall efficiency of fuel cells [1,2]. One effective way to overcome the crossover problem is to adopt methanol-tolerant catalysts as the cathode materials of DMFCs [1]. Because of the sensitivity to methanol and high price of Pt, many researchers have switched to other alternative materials [3,4]. Transition metal macrocycle compounds [5–10], transition metal sulfide [11] and ruthenium-based materials [12–18] have been exploited one after another. Despite their good selectivity against the methanol oxidation reaction, these catalysts have considerably lower activity for the oxygen reduction reaction (ORR) than Pt-based ones. Considering that Pd possesses a similar valence electronic configuration and lattice constant to Pt and yet a highly methanol-tolerant ability [19,20], some researchers begin to devote to the research and development of Pd catalysts as promising cathode materials [21–25]. To further improve the catalytic activity and stability of Pd for the ORR, many metallic elements such as Ti [26], Au [27], Co [28–36], Fe [37], Ni [38], etc. were added into Pd. These metallic elements, however, easily leak into the strong acid electrolyte under electrochemical oxidative conditions. The modification of some non-metals such as Se [39] and P [40] was found to have some positive effect on the catalytic activity of Pd.

It is well known that the support of catalysts plays an important role in the dispersion of metal nanoparticles and the transportation of reactants/products, directly influencing the catalytic activity and stability of catalysts [41–43]. Tungsten oxide as the support of Pt and $RuSe_x$ catalysts has been used to improve their catalytic performance for the ORR [44–46]. It was found that tungsten oxide, due to its interaction with Pt or $RuSe_x$ by the formation of hydrogen tungsten bronze [47], is reactive towards the hydrogen peroxide intermediate.

In this paper, WO_3 was deposited onto the Vulcan XC-72R carbon with the large specific surface area and conductivity to form a hybrid support. Then the palladium was directly reduced onto the hybrid support. The resultant Pd–WO_3/C catalysts were found to greatly improve the catalytic activity of Pd for the ORR. The nature and function of tungsten oxide in the catalyst were also analyzed.

2. Experimental

The WO_3/C hybrid material was prepared as follows. The sodium tungstate as the precursor of WO_3 was added to the suspension of Vulcan XC-72R carbon under vigorous agitation before the solution

* Corresponding author. Tel.: +86 431 85262223; fax: +86 431 85685653.
E-mail address: xingwei@ciac.jl.cn (W. Xing).

0378-7753/$ – see front matter © 2008 Elsevier B.V. All rights reserved.
doi:10.1016/j.jpowsour.2008.07.044

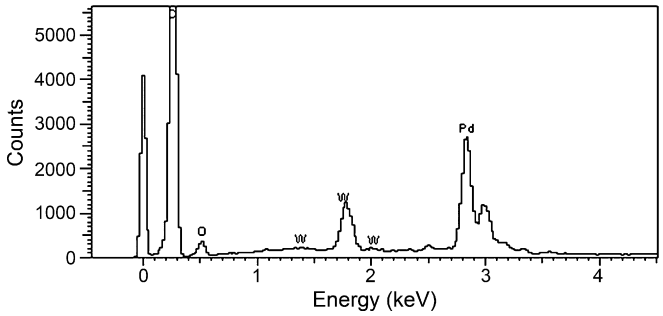

Fig. 1. EDX spectrum of the Pd–WO_3/C catalyst.

was heated to 80 °C. With the addition of excessive hydrochloric acid, the tungstenic acid deposit was formed. After the reaction proceeded for 6 h, the suspension was filtered, washed and dried at 80 °C in a vacuum oven. To obtain stable WO_3/C, the resultant was transferred to a tubular oven and heat-treated at 500 °C for 180 min under the protection of nitrogen.

Pd nanoparticles were deposited onto the WO_3/C by a $NaBH_4$ reduction method. First, an appropriate amount of H_2PdCl_4 aqueous solution was thoroughly mixed with the WO_3/C support by sonication and agitation. Then pH value of the solution was adjusted to ca. 7 by a 5% NaOH solution. Afterward, an excessive $NaBH_4$ solution was added dropwise into the above mixture. Finally, the catalyst was filtered, washed and dried overnight at 80 °C in a vacuum oven. The resultant Pd–WO_3/C catalyst with 20 wt.% Pd and 20 wt.% WO_3 was denoted as the Pd–WO_3/C. For comparison, 20 wt.% Pd/C were prepared with the same method.

The composition of catalysts was estimated by energy dispersive X-ray analysis (EDX) on a JEOL JAX-840 scanning electron microscope operating at 20 kV. The X-ray diffraction (XRD) patterns were obtained using a Rigaku-D/MAX-PC 2500 X-ray diffractometer with the Cu Kα (λ = 1.5405 Å) radiation source operating at 40 kV and 200 mA. X-ray photoelectron spectroscopy (XPS) measurements were carried out using a Kratos XSAM-800 spectrometer with an Mg Kα radiator. The TEM images were recorded on a JEOL 2010 transmission electron microscope operating at 200 kV.

An EG&G Model 273A potentiostat/galvanostat and a conventional three-electrode test cell were used for the electrochemical measurements. The working electrode was a thin layer of Nafion-impregnated catalyst cast on a rotating glassy carbon electrode (5 mm in diameter). Pt gauze and Ag/AgCl electrodes were used as the counter and reference electrodes, respectively. All potentials were quoted against Ag/AgCl. The current density in the electrochemical measurements was normalized to the geometrical surface area of the working electrode.

3. Results and discussion

Fig. 1 shows a typical EDX spectrum of the Pd–WO_3/C catalyst. The composition of the catalyst was found to consist of Pd, W, C and O. The atomic ratio of Pd to W is 3:1. The result confirms that element W exists inside the bulk phase of Pd–WO_3/C catalyst. The absence of chlorine peak indicates that the chlorine ions have been completely removed during the filtration.

The XRD patterns of the Pd/C, Pd–WO_3/C and WO_3/C catalysts are shown in Fig. 2 to analyze their bulk structure. The diffraction peaks at ca. 39°, 46°, 67° and 81° observed in the Pd/C (Fig. 2a) correspond to the face centered cubic (fcc) phase of Pd, while those at ca. 33°, 40°, 49°, 54°, 61° and 76° observed in the WO_3/C (Fig. 2c) correspond to the monoclinic phase of WO_3 [48,49]. The diffraction peaks at 23° observed in the catalysts except for the Pd/C are due to the mixture of the (0 0 2) reflection of Vulcan XC-72 carbon and (0 2 0) reflection of WO_3 [50]. The characteristic peaks of Pd and WO_3 can be observed in the Pd–WO_3/C (Fig. 2b) although they are very small. Therefore, the Pd–WO_3/C catalyst has a separate fcc phase of Pd and monoclinic phase of WO_3.

Fig. 3 shows the XPS spectra of the Pd/C and Pd–WO_3/C catalysts. It can be seen from Fig. 3a that an obvious W peak appears in the W(4f) region of XPS spectra. The W($4f_{7/2}$) and W($4f_{5/2}$) peaks for the Pd–WO_3/C catalyst locate at 34.9 eV and 37.1 eV, respectively, which confirms that W exists in the form of tungsten oxide on the surface of the Pd–WO_3/C catalyst [51]. As shown in Fig. 3b, the binding energies of the C(1s) main peak, Pd($3d_{5/2}$), and Pd($3d_{3/2}$) for the Pd/C catalyst are 284.7 eV, 334.9 eV, and 340.2 eV, respectively, while those for the Pd–WO_3/C catalyst are 284.5 eV, 335.7 eV and 340.6 eV, respectively. To inspect any shift accurately, the binding energies of the Pd(3d) peaks were referred to the C(1s) main peak. It was found from the above XPS comparison that Pd($3d_{5/2}$), and Pd($3d_{3/2}$) peaks shift positively by 1.0 eV and 0.6 eV, respectively, after tungsten oxide is introduced to the Pd/C catalyst. This confirms that a strong "metal-support interaction" exists between Pd and WO_3. This kind of "metal-support interaction" can modify the electronic and catalytic properties of metal nanoparticles and lead to the activation of both dispersed metal and oxide matrix toward electrode processes, which is very necessary for an efficient electrocatalytic system [52].

The TEM images of the Pd/C and Pd–WO_3/C catalysts are presented in Fig. 4. The Pd nanoparticles in the Pd–WO_3/C catalyst were found to disperse more uniformly on the WO_3/C support (Fig. 4b) than on the carbon support alone (Fig. 4a). Moreover, Pd particles in the Pd–WO_3/C catalyst have smaller sizes and a narrower size distribution than those in the Pd/C catalyst. The average size of the Pd nanoparticles in the Pd–WO_3/C catalyst was estimated as ca. 2.5 nm. The TEM demonstrates that the introduction of tungsten oxide inhibits the aggregation of Pd particles, leading to higher dispersion of the Pd nanoparticles and a narrow size distribution, which is supported by the XPS evidence that the strong "metal-support interaction" exists between Pd and WO_3.

Cyclic voltammograms of the Pd/C and Pd–WO_3/C electrocatalysts in 0.5 M H_2SO_4 solution are shown in Fig. 5. The hydrogen desorption peaks of the Pd/C catalyst are located at ca. −0.05 V and 0.05 V, while those of the Pd–WO_3/C catalyst at ca. −0.10 V and 0.05 V. Furthermore, the area of the hydrogen adsorption/desorption peaks of the Pd–WO_3/C catalyst (Fig. 5b)

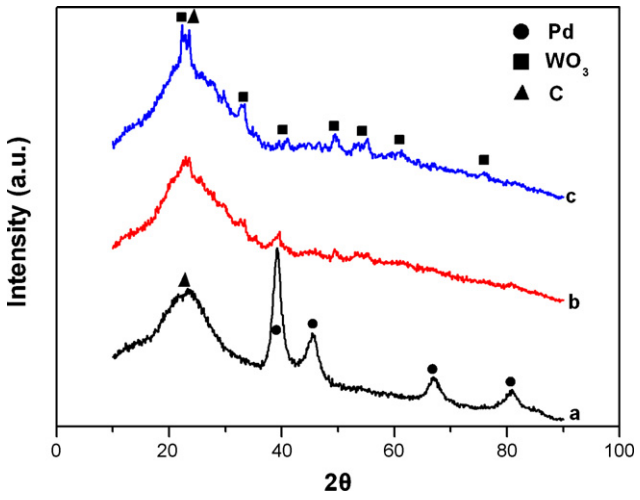

Fig. 2. XRD patterns of (a) the Pd/C, (b) Pd–WO_3/C and (c) WO_3/C catalysts.

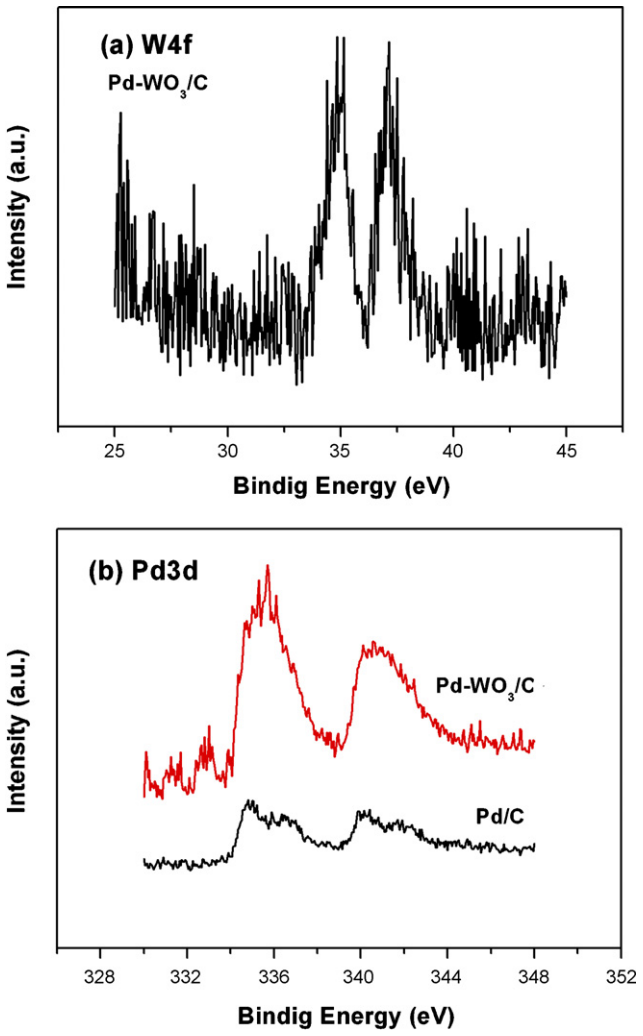

Fig. 3. XPS spectra of the Pd/C and Pd–WO_3/C catalysts: (a) W(4f) region (only for the Pd–WO_3/C catalyst) and (b) Pd(3d) regions.

is much larger than that of the Pd/C catalyst (Fig. 5a), indicating that the Pd–WO_3/C catalyst has larger electrochemical surface area (ESA). On one hand, the larger ESA results from the small particle size of Pd in the Pd–WO_3/C catalyst observed from the TEM results (Fig. 4). On the other hand, this is also associated with the formation of hydrogen tungsten bronze [47]. It has been reported in many literatures that tungsten oxide easily forms hydrogen tungsten bronze by hydrogen intercalation in the hydrogen adsorption region. Ganesan and Lee found that tungsten oxide alone exhibits a broad anodic peak at ca. 0.1 V in 1 M H_2SO_4, which is due to the hydrogen deintercalation of hydrogen tungsten bronze formed in the hydrogen adsorption region [53]. The absence of characteristic peaks of hydrogen tungsten bronze in our Pd–WO_3/C system is likely due to the mask by the stripping of a large quantity of hydrogen in Pd. Hydrogen adsorbed on Pd may spill over onto the surface of WO_3 and form "hydrogen tungsten bronze (H_xWO_3)", thus releasing these Pd active sites for further adsorption of hydrogen. H_xWO_3 can be readily oxidized at a lower potential to release hydrogen ions and WO_3:

$$WO_3 + x\text{Pd–H} \rightarrow H_xWO_3 + x\text{Pd} \quad (1)$$

$$H_xWO_3 \rightarrow WO_3 + xH^+ + xe^- \quad (2)$$

In addition, the peak areas of Pd oxidation and its oxides' reduction on the surface of Pd–WO_3/C catalyst are larger than those on the Pd/C catalyst. Similarly, the oxidation–reduction feature results from the change of particle size in the presence of WO_3.

Fig. 6 shows the linear sweep voltammograms of the Pd/C, Pd–WO_3/C and Pt/C (E-TEK) catalysts in the oxygen-saturated H_2SO_4 solutions. The onset and half-wave potentials for the ORR at the Pd–WO_3/C catalyst are 70 mV and 35 mV more positive than those at the Pd/C catalyst, respectively. This implies that the Pd–WO_3/C catalyst is more active than the Pd/C catalyst. The limiting current density of the Pd–WO_3/C catalyst is significantly larger than that of the Pd/C catalyst and comes up to the level of the commercial Pt/C catalyst (E-TEK) although its ORR potential is less positive than that of the commercial Pt/C catalyst. This means that more oxygen molecules can reach the surface of the Pd–WO_3/C catalyst, which may be due to the larger electrochemical surface area resulting from the smaller particle sizes.

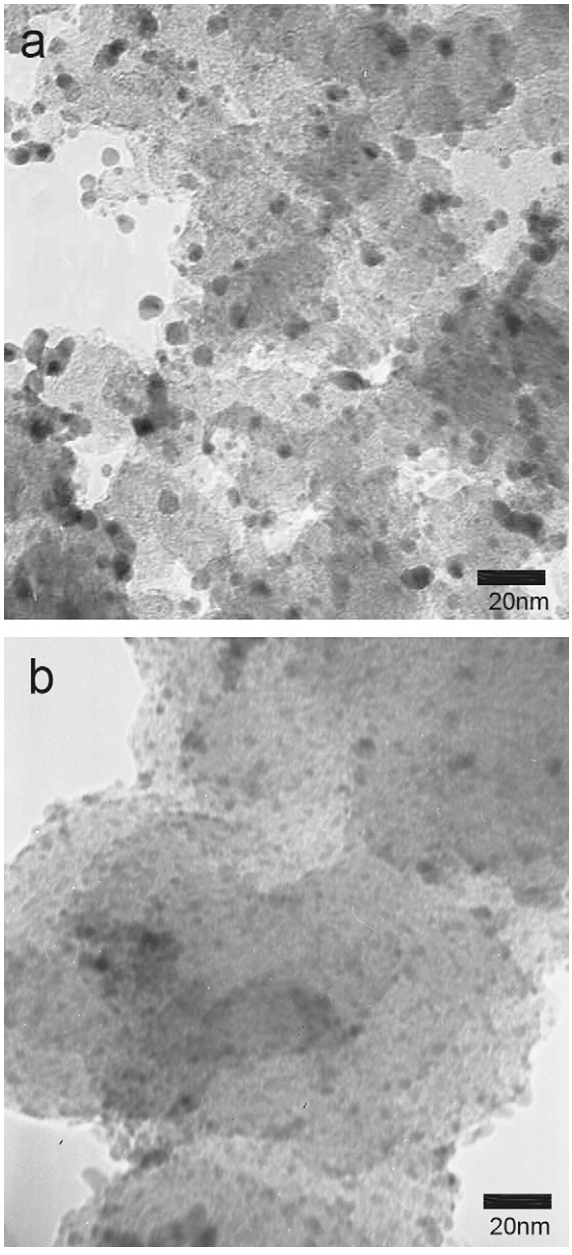

Fig. 4. TEM images of (a) the Pd/C and (b) Pd–WO_3/C catalysts.

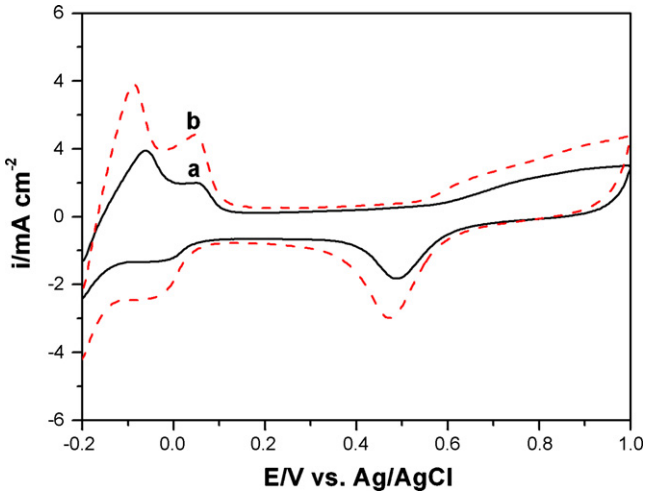

Fig. 5. Cyclic voltammograms of (a) the Pd/C and (b) Pd–WO_3/C catalysts in 0.5 M H_2SO_4 solutions with a scan rate of 50 mV s^{-1}.

So far, no agreement on the ORR mechanism at Pd electrode has been arrived at. If peroxide pathway is present in the ORR, at least an additional hump or small plateau would be expected to appear at a low potential in the linear sweep voltammogram of the ORR. However, it can be found from Fig. 6 that only one plateau appears at ca. 0.45 V at the Pd catalysts. Furthermore, the slope of the curves at the Pd samples is steeper than that at the Pt/C catalyst, indicating that the presence of an intermediate is hardly possible. Therefore, it is likely that the ORR at the Pd sample proceeds mainly through the direct 4-electron pathway. As we know, WO_3 does not possess obvious catalytic activity for the ORR [45]. In addition to the small particle sizes and uniform dispersion of Pd on the WO_3/C, the promotion of WO_3 for Pd catalytic activity may result from two aspects. On one hand, the introduction of WO_3 leads to the positive shift of Pd3d peaks as XPS technique indicates and changes the electronic property of Pd. The strong interaction between WO_3 and Pd may weaken the binding energy between Pd and O atoms, which effectively promotes the direct 4-electron pathway of the ORR at Pd. On the other hand, WO_3 forms "hydrogen tungsten bronze (H_xWO_3)" with the spillover hydrogen (Eq. (1)) and thus increases the conductivity of WO_3 over three orders of magnitude, which allows electrons to be easily conducted to Pd centers that are inactive in the matrix [45]. At the same time, the hydrated H_xWO_3 also facilitates the proton transfer during the ORR (Eq. (2)).

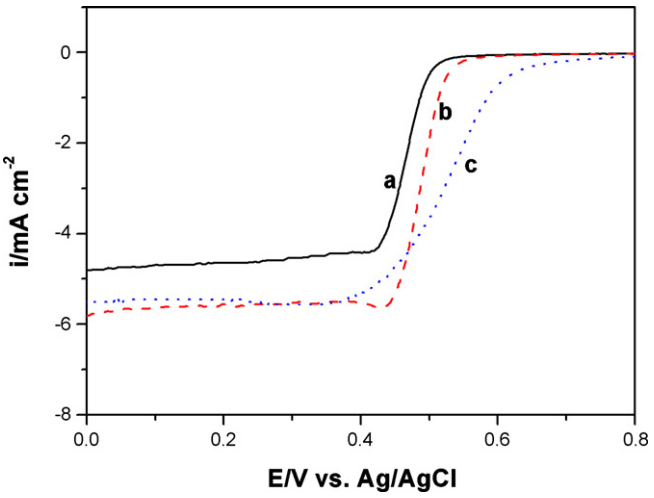

Fig. 6. Linear sweep voltammograms of (a) the Pd/C, (b) Pd–WO_3/C and (c) Pt/C (E-TEK) catalysts in 0.5 M oxygen-saturated H_2SO_4 solutions with a scan rate of 10 mV s^{-1} and a rotation speed of 1500 rpm.

4. Conclusions

In this study, Pd nanoparticles have been loaded on the hybrid material based on WO_3 and Vulcan XC-72R carbon and exhibit a good electrocatalytic activity for the ORR. The EDX, XPS and XRD results indicate that W exists in the form of tungsten oxide not only inside but also on the surface of the Pd–WO_3/C and that the Pd–WO_3/C catalyst has a separate fcc phase of Pd and monoclinic phase of WO_3. XPS also confirms the presence of the strong "metal-support interaction" between Pd and WO_3. TEM shows the small particle sizes and uniform dispersion of Pd on the WO_3/C support. The improvement in the catalytic performance may be attributed to the small particle sizes and uniform dispersion of Pd on the WO_3/C, the strong interaction between Pd and WO_3 and the formation of hydrogen tungsten bronze which effectively promote the direct 4-electron pathway of the ORR at Pd.

Acknowledgements

This project was supported by the State Key Fundamental Research Program of China (973 Program, G2000026408), the State Key High Technology Research Program of China (863 Program, 2001AA323060), and the Nature Science Foundation of China (20373068 and 20433060).

References

[1] B. Bittins-Cattaneo, S. Wasmus, B. Lopez-Mishima, W. Vielstich, J. Appl. Electrochem. 23 (1993) 625.
[2] V. Paganin, E. Sitta, T. Iwasita, W. Vielstich, J. Appl. Electrochem. 35 (2005) 1239.
[3] B. Wang, J. Power Sources 152 (2005) 1.
[4] L. Zhang, J. Zhang, D.P. Wilkinson, H. Wang, J. Power Sources 156 (2006) 171.
[5] M. Lefevre, J.P. Dodelet, P. Bertrand, J. Phys. Chem. B 104 (2000) 11238.
[6] R. Jiang, D. Chu, J. Electrochem. Soc. 147 (2000) 4605.
[7] P. Convert, C. Coutanceau, P. Crouïgneau, F. Gloaguen, C. Lamy, J. Appl. Electrochem. 31 (2001) 945.
[8] M. Lefevre, J.P. Dodelet, P. Bertrand, J. Phys. Chem. B 106 (2002) 8705.
[9] N.A. Savastenko, V. Bruser, M. Bruser, K. Anklam, S. Kutschera, H. Steffen, A. Schmuhl, J. Power Sources 165 (2007) 24.
[10] C.W.B. Bezerra, L. Zhang, H. Liu, K. Lee, A.L.B. Marques, E.P. Marques, H. Wang, J. Zhang, J. Power Sources 173 (2007) 891.
[11] D. Susac, L. Zhu, M. Teo, A. Sode, K.C. Wong, P.C. Wong, R.R. Parsons, D. Bizzotto, K.A.R. Mitchell, S.A. Campbell, J. Phys. Chem. C 111 (2007) 18715.
[12] T.J. Schmidt, U.A. Paulus, H.A. Gasteiger, N. Alonso-Vante, R.J. Behm, J. Electrochem. Soc. 147 (2000) 2620.
[13] M. Bron, P. Bogdanoff, S. Fiechter, I. Dorbandt, M. Hilgendorff, H. Schulenburg, H. Tributsch, J. Electroanal. Chem. 500 (2001) 510.
[14] G. Zehl, G. Schmithals, A. Hoell, S. Haas, C. Hartnig, I. Dorbandt, P. Bogdanoff, S. Fiechter, Angew. Chem. Int. Ed. 46 (2007) 7311.
[15] G. Liu, H. Zhang, J. Hu, Electrochem. Commun. 9 (2007) 2643.
[16] P.K. Babu, A. Lewera, J.H. Chung, R. Hunger, W. Jaegermann, N. Alonso-Vante, A. Wieckowski, E. Oldfield, J. Am. Chem. Soc. 129 (2007) 15140.
[17] C.V. Rao, B. Viswanathan, J. Phys. Chem. C 111 (2007) 16538–16543.
[18] A.A. Serov, M. Min, G. Chai, S. Han, S. Kang, C. Kwak, J. Power Sources 175 (2008) 175.
[19] A. Capon, R. Parsons, J. Electroanal. Chem. 44 (1973) 239.
[20] C. Lamy, Electrochim. Acta 29 (1984) 1581.
[21] X.R. Ye, Y. Lin, C.M. Wai, Chem. Commun. (2003) 642.
[22] X.R. Ye, Y.H. Lin, C.M. Wang, M.H. Engelhard, Y. Wang, C.M. Wai, J. Mater. Chem. 14 (2004) 908.
[23] H. Li, Q. Xin, W. Li, Z. Zhou, L. Jiang, S. Yang, G. Sun, Chem. Commun. (2004) 2776.
[24] Y.H. Lin, X.L. Cui, X.R. Ye, Electrochem. Commun. 7 (2005) 267.
[25] Y.G. Suo, L. Zhuang, J.T. Lu, Angew. Chem. Int. Ed. 46 (2007) 2862.
[26] J.L. Fernandez, V. Raghuveer, A. Manthiram, A.J. Bard, J. Am. Chem. Soc. 127 (2005) 13100.
[27] M. Nie, P.K. Shen, Z. Wei, J. Power Sources 167 (2007) 69.
[28] O. Savadogo, K. Lee, K. Oishi, S. Mitsushima, N. Kamiya, K.I. Ota, Electrochem. Commun. 6 (2004) 105.
[29] V. Raghuveer, A. Manthiram, A.J. Bard, J. Phys. Chem. B 109 (2005) 22909.

[30] M.R. Tarasevich, A.E. Chalykh, V.A. Bogdanovskaya, L.N. Kuznetsova, N.A. Kapustina, B.N. Efremov, M.R. Ehrenburg, L.A. Reznikova, Electrochim. Acta 51 (2006) 4455.
[31] W.E. Mustain, K. Kepler, J. Prakash, Electrochem. Commun. 8 (2006) 406.
[32] W.M. Wang, D. Zheng, C. Du, Z.Q. Zou, X.G. Zhang, B.J. Xia, H. Yang, D.L. Akins, J. Power Sources 167 (2007) 243.
[33] J. Mathiyarasu, K.L.N. Phani, J. Electrochem. Soc. 154 (2007) B1100.
[34] W.E. Mustain, K. Kepler, J. Prakash, Electrochim. Acta 52 (2007) 2102.
[35] L. Zhang, K. Lee, J.J. Zhang, Electrochim. Acta 52 (2007) 3088.
[36] L. Zhang, K. Lee, J. Zhang, Electrochim. Acta 52 (2007) 7964.
[37] M.H. Shao, K. Sasaki, R.R. Adzic, J. Am. Chem. Soc. 128 (2006) 3526.
[38] K. Lee, O. Savadogo, A. Ishihara, S. Mitsushima, N. Kamiya, K.-i. Ota, J. Electrochem. Soc. 153 (2006) A20.
[39] A.A. Serov, S.-Y. Cho, S. Han, M. Min, G. Chai, K.H. Nam, C. Kwak, Electrochem. Commun. 9 (2007) 2041.
[40] L. Cheng, Z. Zhang, W. Niu, G. Xu, L. Zhu, J. Power Sources 182 (2008) 91.
[41] M. Uchida, Y. Aoyama, M. Tanabe, N. Yanagihara, N. Eda, A. Ohta, J. Electrochem. Soc. 142 (1995) 2572.
[42] S.C. Roy, P.A. Christensen, A. Hamnett, K.M. Thomas, V. Trapp, J. Electrochem. Soc. 143 (1996) 3073.
[43] N. Jia, R.B. Martin, Z. Qi, M.C. Lefebvre, P.G. Pickup, Electrochim. Acta 46 (2001) 2863.
[44] P.J. Kulesza, L.R. Faulkner, J. Electroanal. Chem. 259 (1989) 81.
[45] P.J. Kulesza, B. Grzybowska, M.A. Malik, M.T. Galkowski, J. Electrochem. Soc. 144 (1997) 1911.
[46] P.J. Kulesza, K. Miecznikowski, B. Baranowska, M. Skunik, S. Fiechter, P. Bogdanoff, I. Dorbandt, Electrochem. Commun. 8 (2006) 904.
[47] B.S. Hobbs, A.C.C. Tseung, Nature 222 (1969) 556.
[48] T. Maiyalagan, B. Viswanathan, J. Power Sources 175 (2008) 789.
[49] J. Rajeswari, B. Viswanathan, T.K. Varadarajan, Mater. Chem. Phys. 106 (2007) 168.
[50] D.Y. Zhang, Z.F. Ma, G.X. Wang, K. Konstantinov, X.X. Yuan, H.K. Liu, Electrochem, Solid State Lett. 9 (2006) A423.
[51] J.F. Moulder, W.F. Stickle, P.E. Sobol, K.D. Bomben, in: J. Chastain (Ed.), Handbook of X-ray Photoelectron Spectroscopy, Perkin–Elmer Corp., Eden Praire, MN, 1992.
[52] B.C. Beard, J.P.N. Ross, J. Electrochem. Soc. 133 (1986) 1839.
[53] R. Ganesan, J.S. Lee, J. Power Sources 157 (2006) 217.